BIO Web of Conferences **194**, 01085 (2025) https://doi.org/10.1051/bioconf/202519401085
BFT-2025

Numerical simulation of CO_2–liquid droplet separation via membrane filtration and vibration-enhanced droplet spreading

Ivan Volodin[11] and *Alexey* Alabuzhev[1, 2]

[1]Institute of Continuous Media Mechanics UB RAS, 614013 Perm, Russia
[2]Perm State National Research University, 614068 Perm, Russia

Abstract. This study presents numerical simulations of membrane-based mass transfer in a three-layer system and of droplet interface evolution on a solid substrate conducted using the lattice Boltzmann method. The analysis focuses on two key aspects relevant to carbon dioxide filtration in gas–vapor mixtures: flow interactions in multilayer porous systems and droplet spreading under vertical vibrations. Numerical results reveal that increasing the velocity of the upper layer enhances scalar transport across the interface, whereas a higher velocity in the lower layer reduces penetration. Simulations of droplet dynamics demonstrate that vertical vibrational forcing significantly affects spreading behavior and equilibrium shape. Moderate vibrations primarily reduce droplet height, while stronger forcing results in a twofold increase in the wetted area and faster spreading rates. The findings provide a basis for developing advanced models of CO_2 filtration and suggest that both hydrodynamic configuration and dynamic forcing can be used to optimize mass transfer and wetting in multilayer systems.

1 Introduction

Reducing carbon dioxide emissions from fossil fuel combustion is a pressing issue. In most cases, these emissions consist of a mixture of carbon dioxide and water vapor. One promising approach is to condense the vapor and separate the resulting water droplets from carbon dioxide, which has a significantly lower condensation temperature. The behavior of droplets spreading on solid substrates is central to many scientific and technological fields, including microfluidics, diagnostic devices, pharmaceutical analysis, coating, and thin-film processes. The rate of spreading and the final footprint of a droplet directly determine how efficiently reagents, biological samples, or drugs can be delivered, mixed, or detected. Consequently, precise control over wetting dynamics is of particular importance in pharmacology, biophysics, and microfluidics. [1, 2].

In many applications there remains a need to accelerate the spreading (wetting) process further, especially when thin films or small droplets are involved. Methods for controlling the dynamics of droplet spreading using external perturbations, such as mechanical vibrations or acoustic fields, represent an attractive strategy since they do not require modification of

1 Corresponding author: ivanwolodin@gmail.com

the interfacial chemical properties (e.g., application of surface coatings or additives) but instead rely on mechanical excitation. In particular, vertical vibrations (perpendicular to the substrate) can induce oscillations of the contact line, enhance microscopic interfacial deformations, and increase the wetted area on the substrate [3, 4].

In biomedical sciences, the ability to externally control droplet behavior opens new avenues, for example, in the design of advanced drug delivery systems. It allows the creation of well-defined cellular microenvironments, the development of biosensing platforms, and the improvement of lab-on-a-chip devices. Overall, external perturbations represent a flexible and reproducible tool for tuning droplet dynamics, bridging fundamental physics with practical applications in modern pharmacology and biophysics [5, 6]. Fundamental studies on the behavior of bubbles in force fields can be found, for example, in the reviews [7, 8].

This study represents a part of a broader research effort focused on the problem of carbon dioxide filtration in a gas–vapor mixture.The full formulation of the problem involves a multilayer system in which the upper flow is cooled, leading to condensation and droplet formation. In the future, it is proposed to remove these drops by filtering from carbon dioxide, which can then be preserved in some way. In such conditions, it is crucial to account for the spreading dynamics of the droplets and for possible mechanisms to enhance this spreading. Furthermore, since the system is based on a multilayer membrane structure, variations in material properties across the layers must be incorporated into the model.

In the present work, we report a subset of key representative results that form essential components of the overall problem. Specifically, we provide numerical results for flow through a porous medium under different velocity ratios between the layers, considered here in the isothermal regime. In addition, we present 3D numerical simulations of droplet spreading, including cases where vertical vibrations are applied to accelerate the spreading process.

In this study, we employ a lattice Boltzmann simulation (LBM). LBM is an outstanding framework for numerical simulations due to its unique combination of simplicity, flexibility, and efficiency. Unlike traditional computational fluid dynamics (CFD) methods that solve the macroscopic Navier–Stokes equations, LBM models fluid behavior at the mesoscopic scale, tracking the evolution of particle distribution functions on a discrete lattice. LBM is highly parallelizable and well-suited for modern high-performance computing, making it efficient for large-scale simulations and provides both accuracy and flexibility, enabling researchers to model complex fluid systems with relative ease compared to traditional CFD methods [9, 10]. The method is also widely used in problems of electrophoresis, electrowetting, and contact angle measurements [11, 12].

2 Numerical simulation of impurity filtration in a three-layer system

In the first stage, we consider an isothermal problem, assuming that water vapor has already condensed as water droplets in a stream of carbon dioxide. This allows us to demonstrate the feasibility of the filtration method itself. The transport of a passive scalar (water droplets in future researches) in a three-layer system is investigated, where the middle layer is a porous medium and the upper and lower layers are free of any solid matrix (see Fig. 1). The system is subjected to gravity.

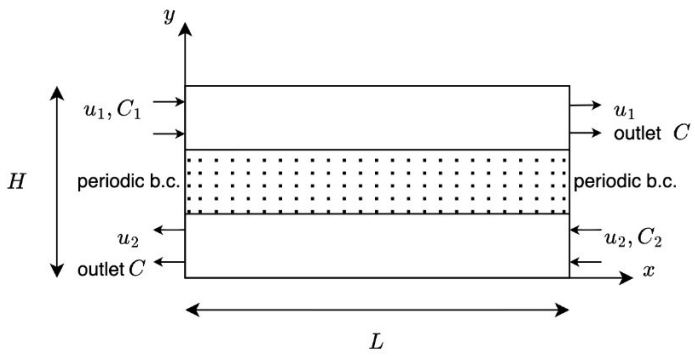

Fig. 1. Problem geometry of three-layer system.

The boundary concentration values are set to $C_1 = 0.5$, $C_2 = 0.0$, and the velocities $\boldsymbol{u_1}$ and $\boldsymbol{u_2}$ have only an x-component. A free-slip boundary condition [9, 10] is imposed on the upper walls for the velocity field. The outlet condition is discussed in [13]. The porosity ε and permeability K are assumed to be uniform and constant. The Darcy number is $Da = K/H^2 = 10^{-2}$, $\varepsilon = 0.5$, the Schmidt number is $Sc = \nu/D = 10^3$, where $\nu$is the kinematic viscosity and D is the diffusion coefficient.

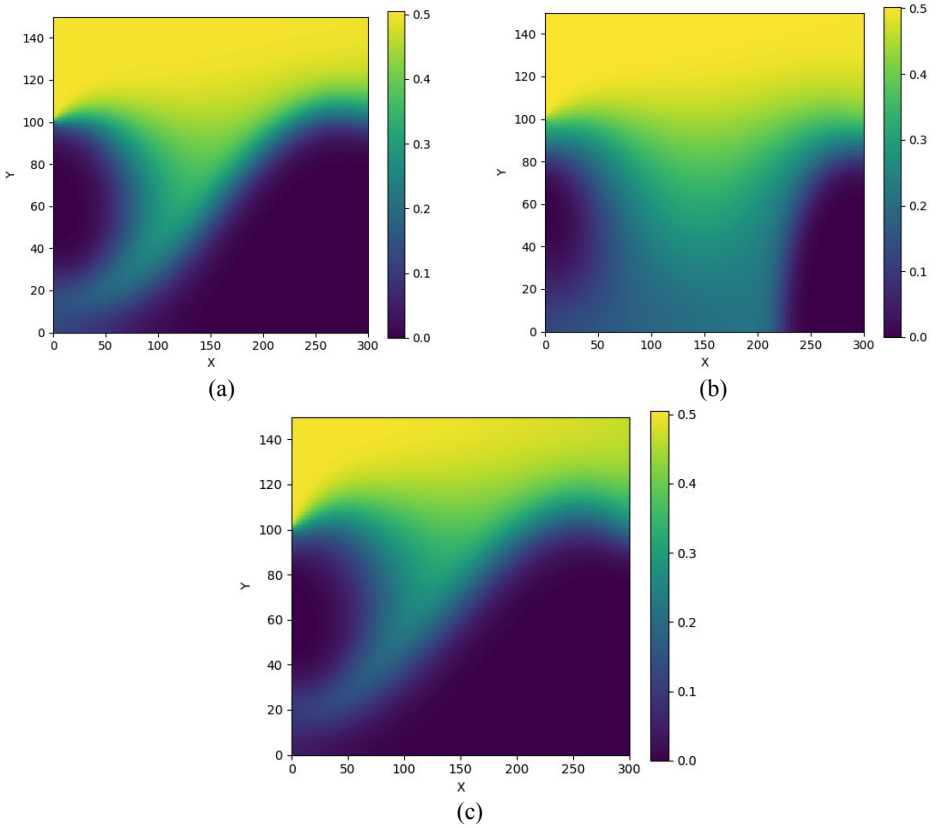

Fig. 2. The steady-state concentration fields for (a) $|\boldsymbol{u_1}| = |\boldsymbol{u_2}|$, (b) $|\boldsymbol{u_1}| = 2|\boldsymbol{u_2}|$, (c) $2|\boldsymbol{u_1}| = |\boldsymbol{u_2}|$

Three cases are considered: $|\boldsymbol{u_1}| = |\boldsymbol{u_2}|$, $2|\boldsymbol{u_1}| = |\boldsymbol{u_2}|$ and $|\boldsymbol{u_1}| = 2|\boldsymbol{u_2}|$. The problem is solved numerically using the lattice Boltzmann method on a D2Q9 lattice with an MRT collision operator. The computational grid consists of $N_x = 300$ nodes in the x -direction and $N_y = 150$ nodes in the y-direction. The details of the numerical algorithm are discussed in [14].

The steady-state concentration fields for the three values of the inlet velocity are shown in Fig. 2. The corresponding steady concentration profiles at $x = N_x/2$ are presented in Fig. 3.

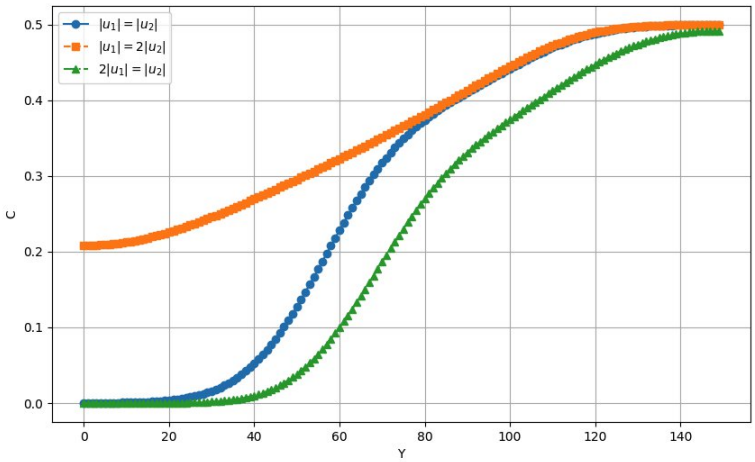

Fig. 3. The steady-state concentration profiles at $x = N_x/2$ for three boundary velocity values

The analysis of the results shows that an increase in the velocity of the upper layer relative to the lower one leads to a substantial enhancement of scalar transport compared to the case of equal velocities (see Fig. 3). Conversely, the weakest penetration of the scalar into the lower layer is observed when the velocity of the lower layer exceeds that of the upper layer, corresponding to the condition $2|\boldsymbol{u_1}| = |\boldsymbol{u_2}|$.

3 Relaxation dynamics of a spherical droplet under periodic vertical vibrations

When studying the formation of liquid droplets during condensation, the spreading of the liquid over a solid surface and its subsequent filtration through a porous structure (such as a membrane) are important processes. Furthermore, droplet spreading and the movement of the contact line enhance liquid flow within the droplet and can, for example, be utilized to improve mixing in microfluidic devices. An external force field (such as vibrations or temperature gradients) can be used to control the droplet and intensify the internal flow. Additionally, both gas and liquid flows can be pulsating.

In the presence of vertical periodic vibrations, the vibrational effect is conventionally represented through a modulation of the effective gravitational acceleration:

$$g(t) = g_0\left(1 + A\sin(\omega t)\right),$$

where g_0 denotes the standard gravitational acceleration, $A = a\omega^2$ – vibrational acceleration, where a and ω are the vibrational amplitude and frequency, respectively. The modulated gravitational acceleration is substituted into equilibrium distribution function (Eq. 4), thereby simulating the effect of vertical vibrations.

The evolution of a spherical droplet spreading on a 100×100 computational grid is examined for a prescribed contact angle of $\theta = 30^\circ$ under vertical vibrations.

The initial droplet profile is given by $h = \sqrt{R^2 - r^2} - R\cos(\theta_{\text{initial}})$, where $R = 20.0$ is a droplet radius in LBM grid units, $\theta_{\text{initial}} = 60^\circ$ is the initial contact angle. The radial distance in the substrate plane was defined as $r^2 = (x - r_x)^2 + (y - r_y)^2$, where $(r_x = N_x/2, r_y = \mathrm{N_y}/2)$ denotes the droplet center. The geometry of the problem is illustrated in Fig. 4.

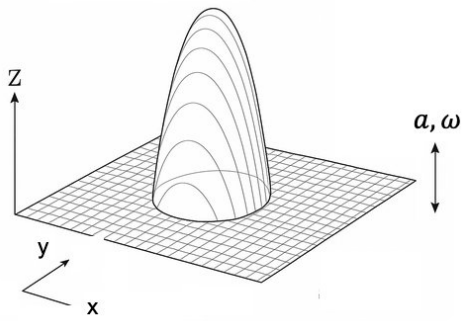

Fig. 4. Sketch of a spherical droplet under periodic vertical vibrations.

The solution was obtained using the lattice Boltzmann method (LBM) within the thin-film approximation [15].

The vibration frequency was set to $\omega = 5.0{\cdot}10^{-2}$, corresponding to approximately 500 Hz in dimensional units. The amplitude was set to $a = 4.0{\cdot}10^4$ and $a = 8.0{\cdot}10^4$, which correspond to dimensional values of 0.4 m and 0.8 m, respectively. Additionally, the case of $a = 0$ was simulated for comparison.

The equilibrium profile shape of the droplet at $y = N_y/2$ is shown in Fig. 5. As can be seen, for a high vibrational acceleration of $A = 200$, the droplet's equilibrium height decreases and spreading becomes more pronounced. In contrast, for $A = 100$, the equilibrium height is lower than in the absence of vibrations ($A = 0$), while the spreading radius remains essentially unchanged.

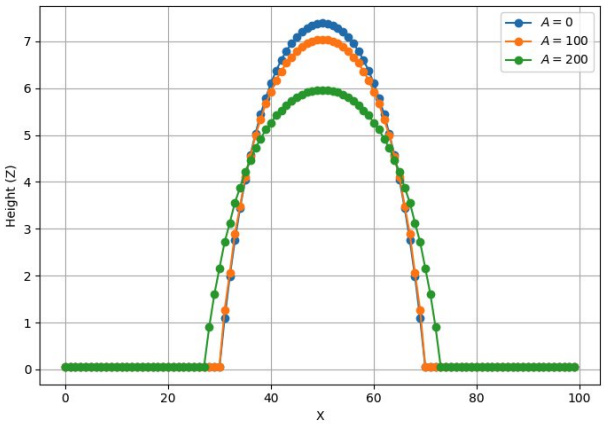

Fig. 5. Profile of the equilibrium droplet shape at $y = N_y/2$ under vertical vibrations.

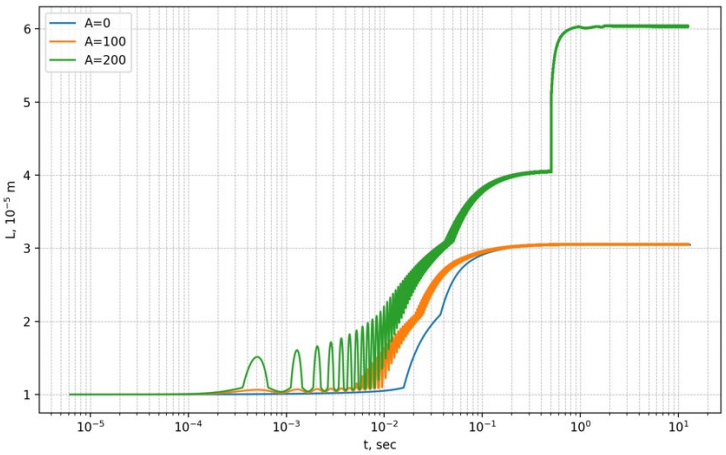

Fig. 6. Time evolution of the droplet radius L at $y = N_y/2$ on the substrate for different values of vibrational acceleration A

The time evolution of the droplet radius L (measured at $y = N_y/2$) on the substrate under different values of vibrational acceleration A in dimensional units is presented in Fig. 6. The horizontal axis is shown in logarithmic scale.

The spreading of a droplet in the absence of external forcing was simulated in [15], where it was demonstrated that the spreading radius follows Tanner's law, $L \sim V^{0.3}\left(\frac{\gamma}{\rho\nu}t\right)^{0.1}$, where V is a droplet volume. In the present work we include the results for $A = 0$ in order to clearly illustrate that the presence of vibrations accelerates both the spreading dynamics and the equilibrium wetted area.

As seen from Fig. 6, the spreading rate increases with increasing A. For relatively small values of A, the equilibrium radius coincides with the case without vibrations, whereas for sufficiently large A, the final spreading radius is approximately doubled.

4 Conclusion

This work presents a numerical simulation of the filtration of liquid droplets in a carbon dioxide flow and the evolution of the liquid droplet interface on a solid substrate using the lattice Boltzmann method. The employed numerical method differs from traditional phase-field or pseudopotential approaches in that the discrete scheme does not explicitly solve the Navier–Stokes and interface equations; instead, it simulates the evolution within the mesoscopic approach and the thin-film approximation.

The conducted study provides essential insights into two key aspects of carbon dioxide filtration in a gas–vapor mixture: flow interaction within a multilayer porous system and droplet spreading dynamics under vibrational forcing. Numerical analysis of the three-layer configuration revealed that the velocity ratio between the layers strongly influences scalar transport efficiency. In particular, increasing the velocity of the upper layer significantly enhances transport across the interface, while a higher velocity in the lower layer suppresses penetration.

The effect of vertical vibrational forcing on the spreading of a spherical droplet has been investigated. The results show that such forcing markedly alters both the spreading dynamics and the equilibrium shape of a droplet on a solid substrate. Relatively small vibrations primarily reduce the droplet height while leaving the final spreading radius largely unchanged, whereas higher vibrational accelerations cause a more pronounced decrease in droplet height accompanied by a twofold increase in the wetted area. The time evolution of the droplet radius further indicates that vibrations accelerate spreading relative to the no vibration case, demonstrating that dynamic forcing can effectively enhance droplet spreading.

In summary, the presented results form an essential foundation for developing an advanced model of carbon dioxide filtration in multilayer systems. They demonstrate that both hydrodynamic configuration and external vibrational control can be used to optimize transport and wetting processes. Future work will extend these findings to non-isothermal regimes with phase transitions, providing a more comprehensive understanding of CO_2 capture efficiency in realistic operating conditions.

Acknowledgments

This work was financially supported by the Russian Science Foundation (project No. 24-21-00379).

References

1. L. Amirifar, M. Besanjideh, R. Nasiri, A. Shamloo, F. Nasrollahi, N. Barros, E. Davoodi, A. Erdem, M. Mahmoodi, V. Hosseini, H. Montazerian, J. Jahangiry, M. Darabi, R. Haghniaz, M. Dokmeci, N. Annabi, S. Ahadian, A. Khademhosseini, Droplet-based microfluidics in biomedical applications. Biofabrication. **14,** 022001 (2022). https://doi.org/10.1088/1758-5090/ac39a9
2. G. Chen, G. Lin, A comprehensive understanding on droplets. Adv. Colloid Interface Sci. **341**, 103490 (2025). https://doi.org/10.1016/j.cis.2025.103490
3. S. Daniel, M.K. Chaudhury, P.-G. de Gennes, Vibration-Actuated Drop Motion on Surfaces for Batch Microfluidic Processes. Langmuir **21**, 4240 (2005). https://doi.org/10.1021/la046886s
4. J. Friend, L. Yeo, Microscale acoustofluidics: Microfluidics driven via acoustics and ultrasonics. Rev. Mod. Phys. **83**, 647 (2011). https://doi.org/10.1103/RevModPhys.83.647

5. T. Trinh, H. Do, N. Nam, T. Dan, K. Trinh, N. Lee, Droplet-Based Microfluidics: Applications in Pharmaceuticals. Pharmaceuticals **16**, 937 (2023). https://doi.org/10.3390/ph16070937
6. A. Fergola, A. Ballesio, F. Frascella, L. Napione, M. Cocuzza, S. Marasso, Droplet Generation and Manipulation in Microfluidics: A Comprehensive Overview of Passive and Active Strategies. Biosensors **15**, 345 (2025). https://doi.org/10.3390/bios15060345
7. H.P. Kavehpour, Coalescence of Drops. Annu. Rev. Fluid Mech. **47**, 245 (2015). https://doi.org/10.1146/annurev-fluid-010814-014720
8. A.Z. Zinchenko, R.H. Davis, Motion of Deformable Drops Through Porous Media. Annu. Rev. Fluid Mech. **49**, 71 (2017). https://doi.org/10.1146/annurev-fluid-010816-060331
9. T. Krüger, H. Kusumaatmaja, A. Kuzmin, O. Shardt, G. Silva, E. Viggen, The Lattice Boltzmann Method (Springer, Cham, 2017). https://doi.org/10.1007/978-3-319-44649-3
10. S. Succi, The Lattice Boltzmann Equation: For Complex States of Flowing Matter (Oxford Univ. Press, Oxford, 2018). https://doi.org/10.1093/oso/9780199592357.001.0001
11. É. Ruiz-Gutiérrez, R. Ledesma-Aguilar, Lattice-Boltzmann Simulations of Electrowetting Phenomena. Langmuir **35**, 4849 (2019). https://doi.org/10.1021/acs.langmuir.9b00098
12. B. Wen, B. Huang, Z. Qin, C. Wang, C. Zhang, Contact angle measurement in lattice Boltzmann method. Comput. Math. Appl. **76**, 1686 (2018). https://doi.org/10.1016/j.camwa.2018.07.021
13. A. D'Orazio, A. Karimipour, R. Ranjbarzadeh, Lattice Boltzmann Modelling of Fluid Flow through Porous Media: A Comparison between Pore-Structure and Representative Elementary Volume Methods. Energies **16**, 5354 (2023). https://doi.org/10.3390/en16145354
14. I. Volodin, A. Alabuzhev, Mass Transfer Simulation In An Inclined Two-Layer Porous Channel By The Lattice Boltzmann Method. Microgravity Sci. Technol. **37**, 5 (2025). https://doi.org/10.1007/s12217-025-10200-9
15. S. Zitz, A. Scagliarini, S. Maddu, A.A. Darhuber, J. Harting, Lattice Boltzmann method for thin-liquid-film hydrodynamics. Phys. Rev. E **100**, 033313 (2019). https://doi.org/10.1103/PhysRevE.100.033313